# A non-equilibrium evaporation model for pure cryogens stored in closed tanks with pressure build-up

## Felipe Huerta, Velisa Vesovic

*Department of Earth Science and Engineering, Imperial College London, London SW7 2AZ, UK*
Tel: +44 7753 983853
Emails: f.huerta-perez17@imperial.ac.uk, v.vesovic@imperial.ac.uk

## 1. Introduction

Cryogenic liquids are fluids with a boiling temperature lower than 160°C at atmospheric pressure. These liquids are stored in highly insulated tanks, where despite the high insulation, there is a continuous heat ingress which heats and evaporates the cryogen. One industrial application is the storage of liquefied natural gas (LNG) in large tanks, where the evaporated cryogen is removed, as it is generated, to keep the tank pressure constant; the removed vapour is denominated boil-off gas (BOG). In this scenario, the liquid cryogen is nearly isothermal, and recent evidence has shown vapour superheating between 15K and 100K depending on the tank liquid filling[1, 2]. Evidence of vapour superheating has inspired the development of non-equilibrium models [1, 3, 4], which remove the assumption that all the vapour heat ingress is transferred to the liquid instantly, and consider the vapour phase as a separate heat source.

For liquid cryogen that is highly valuable and cannot be vented to the atmosphere, such as liquid hydrogen in aerospace explorations, pressure builds up within the storage tank and more complex transport phenomena become relevant. The tank pressure rises as a consequence of the evaporation and vapour heating. The pressurization increases the cryogen boiling temperature, at the vapour-liquid interface, producing liquid thermal stratification and affecting the evaporation rates. If the pressure rise is rapid enough, the increase in interfacial temperature can be fast enough to turn evaporation into condensation[5, 6]. The aim of this work is to develop a CFD model which is able to predict liquid thermal stratification, self-pressurization and evaporation rates during the storage of liquid cryogens in small cylindrical closed vessels. The model was developed in OpenFOAM as it provides robust solvers for the Navier Stokes equations and it enables the modification of the source code to simulate novel physical phenomena. A customized solver based on buoyantBoussinesqPimpleFoam, as well as custom boundary conditions to represent the coupling of the vapour pressure with liquid interface temperature were developed. Numerical results showed good agreement when validated against the liquid nitrogen experimental data published by Seo et al. [7], with absolute average deviations (AAD) lower than 4% for pressure and 1% for liquid temperatures.

## 2. Model development

### 2.1 Physical model

The cylindrical storage tank which has been modelled is depicted in Fig.1. The vapour and liquid have been assumed to be separated by a smooth horizontal interface. The vapour is heated by heat transfer through the walls and roof, at a rate $\dot{Q}_V$ and $\dot{Q}_{roof}$, respectively. The liquid is heated through the walls and tank bottom, at a rate $\dot{Q}_L$ and $\dot{Q}_b$, respectively. Additionally, the vapour heats the liquid interface at a vapour to interface heat transfer rate $\dot{Q}_{VI}$. The wall heating in both liquid and vapour phases induces a buoyancy driven flow. Near the tank walls, thin boundary layers for the liquid, $\delta_{BL}^L$, and the vapour, $\delta_{BL}^V$, are formed. At the liquid-vapour interface, the vapour and liquid are assumed in thermodynamic equilibrium at a temperature corresponding to the saturation temperature of the cryogen at the a given vapour pressure. As the vapour is heated, its pressure increases which causes the increase in the vapour-liquid interfacial temperature. The change in the liquid interface temperature occurs much faster than the heat transfer in the liquid bulk, which in conjunction with the buoyancy driven flow, produces a vertical thermal stratification. The liquid cryogen will evaporate or condense, depending on the sign of the net heat flux at the interface, at a rate $\dot{B}_L$, which was defined positive for evaporation and negative for condensation. Both mechanisms can happen at different stages during the storage of the cryogen in the closed tank.
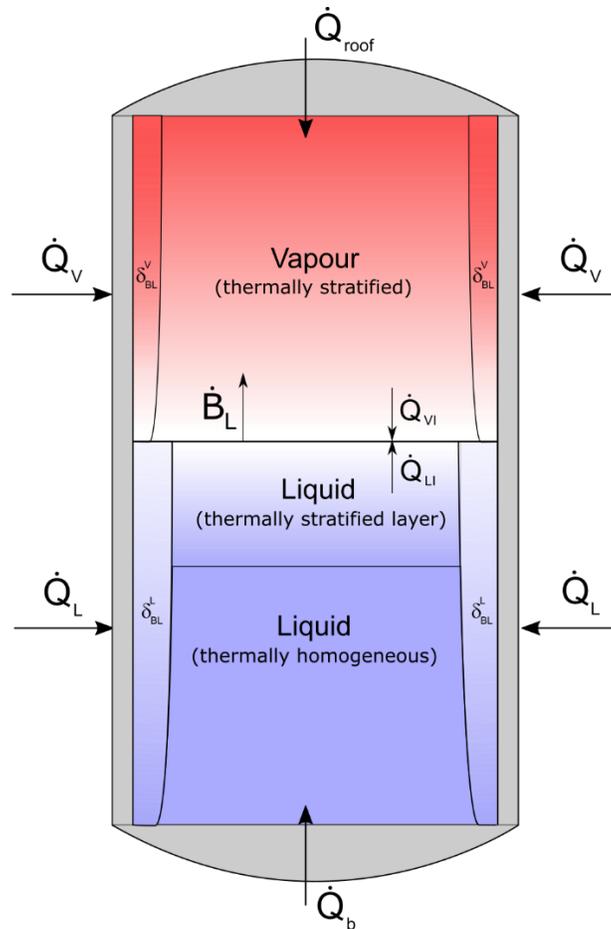
**Figure 1:** Schematic of the modelled closed cryogenic storage tank, where the vapour and the liquid subsystems were assumed to be separated by a smooth, horizontal surface.

Recent numerical results on liquid hydrogen evaporation in small closed vessels suggests that the vapour to interface heat transfer rate, $\dot{Q}_{VI}$, has a small effect on self-pressurization rates and liquid thermal stratification [6]. On the basis of those findings, in this work the vapour phase was simplified and considered spatially homogeneous. As a starting point, the vapour phase was modelled using the vapour bulk model developed by Panzarella et al. [5] for the evaporation of cryogenic liquids in closed vessels. The vapour pressure, temperature and density were assumed spatially homogeneous. The vapour was assumed as an ideal gas, and its molar density is given by:

$$\rho_V = \frac{P_V}{RT_V}, \tag{1}$$

where $P_V$ is the vapour pressure, $R$ is the gas constant and $T_V$ the vapour temperature. As the tank is closed, performing a mass balance on the whole tank yields that total mass of the cryogen in the tank is conserved,

$$\frac{d}{dt}(\rho_V V_V) = -\frac{d}{dt}(\rho_L V_L) \stackrel{\text{def}}{=} \dot{B}_L \,, \tag{2}$$

where $V$ is the volume, $\rho$ is the density and the subscripts L and V indicate liquid and vapour phases, respectively. As the tank volume is fixed, the increase in the volume of any phase must be balanced by the decrease in the volume of the other phase, $dV_V/dt = -dV_L/dt$. The energy balance in the vapour phase bulk was performed by treating the internal energy and the pressure work exerted by the evaporative flow and vapour expansion/compression separately,

$$\frac{d}{dt}(\rho_V V_V c_V T_V) = \dot{Q}_V + \dot{Q}_{\text{roof}} - \dot{Q}_{VI} + \dot{B}_L\left(c_V T_V + \frac{P_V}{\rho_V}\right) - P_V \frac{dV_V}{dt} \,, \tag{3}$$

where $c_V$ is the vapour heat capacity at constant volume. The evaporation rate is governed by an energy balance at the vapour-liquid interface:

$$\dot{B}_L = \frac{(\dot{Q}_{VI} + \dot{Q}_{LI})}{\Delta H_{LV}} \,, \tag{4}$$

where $\Delta H_{LV}$ is the latent heat of vaporization of the cryogen which was assumed constant. This is a good and sensible approximation if the cryogenic fluid thermodynamic properties are far from their critical point. The vapour to interface heat flux was assumed negligible, $\dot{Q}_{VI} = 0$, and the liquid to interface heat ingress was calculated from the liquid temperature field using the Fourier's law,

$$\dot{Q}_{LI} = \int_I \boldsymbol{q}_L \cdot \boldsymbol{n} dS = -\int_I k_{LI} \frac{\partial T_L}{\partial z} dS \,, \tag{5}$$

where $k_{LI}$ is the liquid phase thermal conductivity immediately below the vapour-liquid interface. The ODE system (2)-(3) can be written as an explicit ODE for vapour pressure [5],

$$\frac{dP_V}{dt} = F\left(\dot{Q}_V + \dot{Q}_{\text{roof}} + \dot{Q}_{LI}\right), \tag{6}$$

where $F$ is given by

$$F(P_V) = \frac{\Delta H_{LV}}{V_V}\left(c_V T_S + \left(\frac{\Delta H_{LV} \dot{B}_L}{R T_S} - 1\right)\frac{\rho_L}{\rho_L - \rho_V}\left[\Delta H_{LV} - P_V\left(\frac{1}{\rho_V} - \frac{1}{\rho_L}\right)\right]\right)^{-1}. \tag{7}$$

where $T_S$ is the saturation temperature of the cryogen at the vapour pressure and density. Note that the vapour density is also evaluated at the saturation pressure $P_V$ because the vapour was assumed spatially homogeneous and at physicochemical equilibrium with the liquid at the interface.

The liquid cryogen was assumed incompressible and modelled as a two-dimensional continuum field in the cylindrical domain $\Omega = [0, R_t] \times [0, l_L]$, where $R_t$ is the tank radius and $l_L$ the height of the liquid phase. The velocity, pressure and temperature fields were modelled using the incompressible Navier-Stokes equations with the Boussinesq approximation to consider the buoyancy driven flow. Turbulence was modelled using the standard $k - \epsilon$ model, based on the standard coefficients and the boundary conditions specified in the OpenFOAM "hotRoom" tutorial [8] . The liquid height was assumed fixed, based on the fact that for short storage times the change in liquid volume is small and the hydrodynamics of the liquid phase does not change significantly with small liquid height changes. The velocity boundary conditions were defined as no-slip at the tank bottom, tank wall in contact with the liquid and at the vapour-liquid interfaces. As all velocity boundary conditions were prescribed, the pressure boundary conditions were calculated. The temperature initial and boundary conditions were defined as:

$$T_L|_{t=0} = T_S(P_{V0}) \tag{8}$$

$$k_L \frac{\partial T_L}{\partial z}|_{z=0,r} = \dot{q}_b = U_b\left(T_{air} - T_L|_{z=0,r}\right), \tag{9}$$

$$k_L \frac{\partial T_L}{\partial r}|_{z=,r=R_t} = \dot{q}_w = U_w\left(T_{air} - T_L|_{z,r}\right), \tag{10}$$

$$T_L|_{z=l_L,r} = T_S(P_V) . \tag{11}$$

$$\frac{\partial T_L}{\partial r}|_{z,r=0} = 0 , \tag{12}$$

where $T_L$ is the liquid temperature, $\dot{q}_b$ is the bottom heat flux, $P_{V0}$ the initial vapour pressure and $U$ is the overall heat transfer coefficient of the tank bottom wall (subscript b) and of the tank cylindrical wall (subscript w). The boundary condition at the liquid interface, Eq. (11), depends on the vapour pressure, which in turn depends on the liquid temperature profile, see Eqs. (5) and (6). This way the vapour and liquid phases are coupled. The developed model of cryogenic evaporation consists of a system of ODEs for the vapour, Eqs. (1)-(7), coupled with the liquid phase incompressible Navier-Stokes equations.

*2.2 Numerical methods and OpenFOAM implementation*

The model was implemented in OpenFOAM v1806. A 2D cylindrical geometry was chosen to solve the Navier Stokes equations in the liquid phase, under the assumption that liquid temperature and velocity changes in the azimuthal direction are negligible. A non-uniform wedge mesh refined in the domain boundaries was created using an in-house developed Gmsh [9] script. The grid size was defined with an aspect ratio of 1 for both the radial and axial discretization ($\Delta r = \Delta z = 0.5$mm). The local refinement was performed using Gmsh bump function with parameter 0.2 in both radial and axial directions. We chose a time-step of 0.1s predicted consistent results, and the difference in the velocity and temperature profile was less than 1% when compared against a timestep of 0.01s. Time was discretized using pure CrankNicolson. The discretization schemes for gradients and Laplacian terms were chosen as Gauss linear and Gauss linear uncorrected, respectively. For the advective terms, the linearUpwind discretization was used for all velocity, temperature and turbulent terms, while the temperature diffusive term was discretized using the Gauss linear scheme.

A customized solver, buoyantBoussinesqPvapFoam, was created based on buoyantBoussinesqPimpleFoam to couple the liquid PDE system with the vapour bulk phase ODE system. An OpenFOAM ODE object is created to solve the ODE system using the RK45 time integration method. The solver uses a sequential approach. First, the liquid field equations are solved. Then, using the temperature gradients at the liquid interface, $\dot{Q}_{\mathrm{LI}}$ is computed using Eq. (5). After obtaining $\dot{Q}_{\mathrm{LI}}$ on that time-step, the evaporation rate can be easily calculated, and the vapour quantities are updated from the previous time-step. Finally, the vapour pressure ODE is solved to provide the vapour pressure for the next time-step. The liquid boundary condition at the interface, Eq. (11), was implemented as a codedFixedValue dynamic code, in the temperature initial and boundary conditions dictionary. At each time-step, the code obtains the vapour pressure, $P_{\mathrm{V}}$, and sets the interface temperature using the Antoine's equation. The Robin boundary conditions for the liquid at the tank bottom and tank roof, Eqs. (9) and (10), are implemented as a codedMixed dynamic code. Owing to the simplifications in the model and the mesh size, the code was efficient and was able to simulate one hour of evaporation in one hour CPU time.

## Results

The model was tested against the Seo et al. experimental results [7] for the evaporation of pure nitrogen in a 6.75L cylindrical tank ($R_t = 0.1005$ m). The heat transfer coefficient was fixed based on the reported liquid fillings (LF) and heat transfer rates ($\dot{Q}$). Fig. 2 compares the pressure predicted by the model with the experimental results for three different cases: low ($LF = 30\%, \dot{Q} = 1.0$W), intermediate ($LF = 50\%, \dot{Q} = 1.2$W) and high ($LF = 70\%, \dot{Q} = 2.5$W) liquid fillings. Good agreement can be observed in all cases. The average absolute deviations (AAD) and maximum deviations (MD) were small for low (AAD = 2.5%, MD = 0.9%), intermediate (AAD = 1.1%, MD = 2.2%) and high (AAD = 2.0%, MD = 3.6%) liquid fillings. For low an intermediate liquid filling, as time progresses the model slightly overpredicts the pressurization rate. This positive bias is expected, as neglecting the vapour to liquid heat transfer and considering the vapour to be thermally homogeneous will increase the evaporation rate and vapour pressure, see Eqs. (6)-(7). On the other hand, at high liquid filling the model underpredicts the evaporation rate at early times, and the error decreases with time. This negative bias can be explained because at large liquid fillings, neglecting the liquid thermal expansion will cause the overprediction of the vapour volume, which will tend to underpredict pressurization rates. As time progresses, the positive bias in the pressurization rate caused by simplified model of the vapour phase seems to balance the negative bias of neglecting liquid thermal expansion.
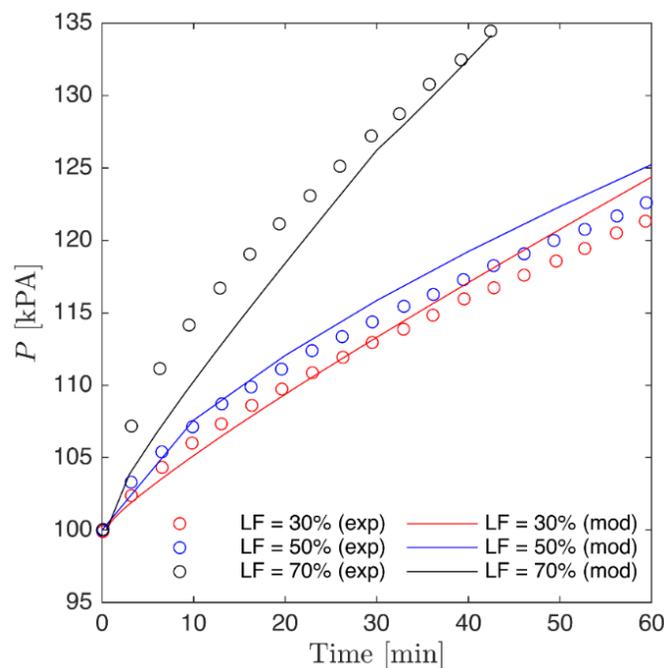


**Figure 2:** Vapour pressure as a function of time for the evaporation of liquid nitrogen stored in a small storage vessel at three different liquid fillings. (----) numerical model and (o) experimental results from Seo et al. [7]

The model also was able to predict liquid temperatures with high accuracy. As the liquid temperature spatial-temporal experimental data was scarcer and showed high experimental error, two representative temperatures were chosen to be compared. The temperature at the bottom of the tank, $T_b$, was assumed to characterize the bulk liquid temperature, while the temperature at the interface, $T_i$, was chosen as a measure of thermal stratification. For the case of LF = 30%, the percentage deviation between the experimental and numerical results for $T_b$ and $T_i$ increased monotonically with time reaching 0.6% and 0.8% at $t = 60$ min, respectively.

## 4. Conclusions

A model for the storage of pure cryogens in closed tanks has been developed. The vapour phase was modelled as a bulk phase, while the liquid phase was modelled as a continuum 2D field governed by the incompressible Navier-Stokes equations with the Boussinesq approximation. The model showed good agreement with liquid nitrogen experimental data for both pressurization rates (AAD < 5%) and liquid temperatures (AAD < 1%) for one hour of storage. We found that modelling the vapour as a bulk phase does not compromise significantly the accuracy of the model in liquid thermal stratification and self-pressurization rates. Furthermore, it enables the use of higher time-steps and coarser meshes, relaxing the need of a multiphase model.

For the conference presentation, a more realistic vapour heat transfer model will be also presented that represents the vapour to liquid heat transfer rate more accurately, and that takes into account the liquid thermal expansion. The vapour phase heat transfer model is expected not to require the solution of the 2D Navier Stokes equation in the vapour phase. Instead, a vapour to liquid heat transfer rate will be estimated at each time-step, from the heat transfer coefficient, evaporation rate and vapour height.

**References**

[1]     S. Effendy, M. S. Khan, S. Farooq, and I. A. Karimi, "Dynamic modelling and optimization of an LNG storage tank in a regasification terminal with semi-analytical solutions for N2-free LNG," *Computers & Chemical Engineering,* vol. 99, pp. 40-50, 2017, doi: 10.1016/j.compchemeng.2017.01.012.

[2]     R. N. Krikkis, "A thermodynamic and heat transfer model for LNG ageing during ship transportation. Towards an efficient boil-off gas management," *Cryogenics,* vol. 92, pp. 76-83, 2018/06/01/ 2018, doi: https://doi.org/10.1016/j.cryogenics.2018.04.007.

[3]     C. Migliore, A. Salehi, and V. Vesovic, "A non-equilibrium approach to modelling the weathering of stored Liquefied Natural Gas (LNG)," *Energy,* vol. 124, pp. 684-692, 2017, doi: 10.1016/j.energy.2017.02.068.

[4]     F. Huerta and V. Vesovic, "A realistic vapour phase heat transfer model for the weathering of LNG stored in large tanks," *Energy,* 2019/02/26/ 2019, doi: https://doi.org/10.1016/j.energy.2019.02.174.

[5]     C. H. Panzarella and M. Kassemi, "On the validity of purely thermodynamic descriptions of two-phase cryogenic fluid storage," *Journal of Fluid Mechanics,* vol. 484, pp. 41-68, 2003, doi: 10.1017/s0022112003004002.

[6]     R. Zhou, W. Zhu, Z. Hu, S. Wang, H. Xie, and X. Zhang, "Simulations on effects of rated ullage pressure on the evaporation rate of liquid hydrogen tank," *International Journal of Heat and Mass Transfer,* vol. 134, pp. 842-851, 2019/05/01/ 2019, doi: https://doi.org/10.1016/j.ijheatmasstransfer.2019.01.091.

[7]     M. Seo and S. Jeong, "Analysis of self-pressurization phenomenon of cryogenic fluid storage tank with thermal diffusion model," *Cryogenics,* vol. 50, no. 9, pp. 549-555, Sep 2010, doi: 10.1016/j.cryogenics.2010.02.021.

[8]     "OpenFOAM v1806, hotRoom tutorial." https://develop.openfoam.com/Development/OpenFOAM-plus/tree/3c3cf51f6977dd110d9932e10e5a0d6b45190342/tutorials/heatTransfer/buoyantBoussinesqSimpleFoam/hotRoom (accessed 25/05/2019.

[9]     C. Geuzaine and J.-F. Remacle, "Gmsh: A 3-D finite element mesh generator with built-in pre- and post-processing facilities," *International Journal for Numerical Methods in Engineering,* vol. 79, no. 11, pp. 1309-1331, 2009/09/10 2009, doi: 10.1002/nme.2579.